RADIAL LOSSES IN HIGH β MULTIPLE MIRROR PLASMAS

by

M. Tuszewski and M. A. Lieberman

Memorandum No. UCB/ERL M79/27

12 March, 1979

ELECTRONICS RESEARCH LABORATORY

College of Engineering
University of California, Berkeley
94704

RADIAL LOSSES IN HIGH β MULTIPLE MIRROR PLASMAS

M. Tuszewski and M. A. Lieberman

Department of Electrical Engineering and Computer Sciences

and the Electronics Research Laboratory

University of California

Berkeley CA 94720

ABSTRACT

The importance of radial losses in collisional multiple mirror confinement is investigated for arbitrary values of β. Classical radial diffusion and complete MHD stability are assumed. Analytical and numerical solutions of the coupled axial and radial diffusion problem are found. The results can be characterized in terms of a single parameter $\alpha \sim (\tau_z/\tau_x)^{\frac{1}{2}}$ where τ_z and τ_x are average values of the axial and radial confinement times. Radial losses are unimportant for $\alpha \lesssim 0.5$ and improvement in overall confinement can be achieved by increasing β for these small values of α. When applied to existing reactor designs, the theory shows that radial losses are important for one-component reactors but can be made negligible for two-component (wetwood burner) reactors.

I. INTRODUCTION

Multiple mirror confinement devices have been considered as possible fusion reactors [1-4]. A multiple mirror consists of a series of connected magnetic mirrors, as shown in Fig. 1. It has been shown [5,6] that in the appropriate plasma density and temperature regime for which the ion mean free path λ is of the same order as the cell length ℓ_c, the axial losses are diffusive with a loss time scaling as L^2, where L is the device length. Reactor designs with moderate lengths and high β have been presented [1,3,4]. However the requirement that λ be small implies a collisional plasma[1] for which radial losses may be significant. A detailed analysis of these transverse losses has not yet been made. In Sect. II of this paper we evaluate quantitatively the relative importance of radial losses compared to axial losses for arbitrary values of the plasma β by finding analytical and numerical solutions to the coupled axial and radial diffusion problem. The theory yields radial and axial profiles at given values of β. Then, In Sec. III we determine quantitatively the relative importance of radial losses for a given system and find qualitative conditions under which higher values of β, which increase radial losses as well as decrease axial losses, can allow more favorable reactor parameters [3]. We then apply the results of the analysis to previous reactor designs [1,3,4].

II. THEORY

We consider the system of Yang and Lieberman [3]. A source S (particles/sec) injects particles at the center $z=0$ of a symmetric system of length L. The source maintains a steady state against radial loss with diffusion coefficient D_x and axial multiple mirror loss with diffusion coefficient D_z. Azimuthal symmetry is assumed. In this two-dimensional system, we use Cartesian (x,z) variables for simplicity. We assume classical ambipolar radial losses with $D_x = a_e^2 \nu_{ei}$ and will support this assumption later. Ambipolar electric field effects are included in D_z by a simple correction factor. We assume an isothermal system with T_e and T_i independent of x and z and a constant practical value for the magnetic field B_{max} in all mirror throats. The density $n(x,z)$ is taken as

$$n(x,z) = n_o(z) \cdot y(x,z) \quad , \quad \text{with} \quad y(0,z) = 1 \tag{1}$$

where n_o refers to the center line density and y gives the radial density variation. The vacuum plasma β is related to n and to the vacuum magnetic field $B_v(z)$ as

$$\beta = \frac{2n(x,z)T}{B_v^2/2\mu_o} \tag{2}$$

We assume a reactor model with a constant centerline value β_o of the plasma β in all mirror midplanes. From Eqs. (1) and (2)

$$\frac{n_o}{B_v^2} = \text{const.} \tag{3}$$

$$\beta = \beta_o y \tag{4}$$

From the vacuum mirror ratio $M_v = B_{max}/B_v$, we get

$$M_v^2 n_o = \text{const.} \tag{5}$$

The plasma radius x_p and B_v are related from flux conservation by

$$B_v x_p^2 = \text{const.} \tag{6}$$

We fix the mean free path regime at the same optimum value [1,3] in all cells by varying the cell length $\ell_c(z)$ as

$$\ell_c = \frac{4\lambda}{M} \tag{7}$$

where λ is the ion-ion (90°) mean free path. We get then

$$D_z = p \frac{\lambda \bar{v}}{M^2} \tag{8}$$

where p is a constant factor which comes from averaging over a Maxwellian distribution and including ambipolar effects [1], and $\bar{v} = (8kT_i/\pi m_i)^{\frac{1}{2}}$. In Eqs. (7) and (8), M is the effective mirror ratio

$$M = M_v \left(\frac{1 - \beta/M_v^2}{1 - \beta} \right)^{\frac{1}{2}} \tag{9}$$

For the values of M_v of interest (e.g., $M_v \gtrsim 1.5$), the factor $(1-\beta/M_v^2)$ varies slowly with β. We take for this factor a constant value $s = (1-\bar{\beta}/M_v^2)$ where $\bar{\beta}$ is the radial averaged β. Eqs. (8) and (9) then give

$$D_z = a \frac{(1 - \beta_o y)}{y} \tag{10}$$

with

$$a = \frac{p\bar{\nu}(\lambda n)}{s(n_o M_v^2)} \tag{11}$$

Similarly, the radial diffusion coefficient D_x can be expressed as

$$D_x = b \frac{y}{1 - \beta_o y} \tag{12}$$

where

$$b = \left(a_e B\right)^2 \cdot \left(\frac{\nu_{ei}}{n}\right) \cdot \left(\frac{n_o}{B_v^2}\right) \tag{13}$$

The continuity equation is

$$\frac{\partial}{\partial z}\left(D_z \frac{\partial n}{\partial z}\right) + \frac{\partial}{\partial x}\left(D_x \frac{\partial n}{\partial x}\right) = 0 \tag{14}$$

Using Eqs. (1), (12) and (13), we get

$$\frac{\partial}{\partial x}\left(\frac{y}{1 - y\beta_o} \frac{\partial y}{\partial x}\right) = - \frac{a}{b} \frac{1}{n_o} \frac{\partial}{\partial z}\left(\frac{1 - y\beta_o}{y} \cdot \frac{\partial (n_o y)}{\partial z}\right) \tag{15}$$

We now assume $\frac{1}{y}\frac{\partial y}{\partial z} \ll \frac{1}{n_o}\frac{\partial n_o}{\partial z}$ since the z dependence of $y(x,z)$ comes only through the plasma radius $x_p \sim n_o^{-\frac{1}{4}}$ as seen from Eqs. (3) and (6).

This assumption can be verified once the radial profile $y(x,z)$ is obtained. For the profiles presented here and especially for $\beta_o \gtrsim 0.8$, the assumption is found justified, e.g., $\frac{1}{y}\frac{\partial y}{\partial z}\Big/\frac{1}{n_o}\frac{\partial n_o}{\partial z} \lesssim 0.1$ over the entire cross-section, except in the neighborhood of the plasma edge where $y \to 0$ and the diffusion analysis breaks down.

Equation (15) then separates into

$$\frac{1}{1-y\beta_o}\cdot\frac{\partial}{\partial x}\left(\frac{y}{1-y\beta_o}\frac{\partial y}{\partial x}\right) = -\, f^2(z) \tag{16}$$

with

$$f^2(z) = \frac{a}{b}\cdot\frac{1}{n_o}\cdot\frac{d^2 n_o}{dz^2} \tag{17}$$

Eq. (16) can be integrated twice. We get first

$$\left(\frac{y}{1-y\beta_o}\right)\frac{\partial y}{\partial x} = -\, f\left(1-y^2\right)^{\frac{1}{2}}$$

where the boundary condition $\left.\frac{\partial y}{\partial x}\right|_{x=0} = 0$ has been used. Then, integrating a second time with the boundary condition $y(0,z) = 1$, we obtain the radial profile in implicit form

$$\arcsin y + \frac{1}{\sqrt{1-\beta_o^2}}\arcsin\left(\frac{\beta_o - y}{1-y\beta_o}\right) = \beta_o f x - \frac{\pi}{2}\left(\frac{1}{\sqrt{1-\beta_o^2}} - 1\right) \tag{19}$$

The z dependence of y, contained in $f(z)$, is related to the plasma radius $x_p(z)$ by $y(x_p,z) = 0$, so that Eq. (19) gives

$$f = \frac{g}{x_p} \tag{20}$$

where g is a function of β_o only given by

$$g = \frac{1}{\beta_o}\left[\frac{1}{\sqrt{1-\beta_o}} \arcsin \beta_o + \frac{\pi}{2}\left(\frac{1}{\sqrt{1-\beta_o}} - 1\right)\right] \tag{21}$$

In Fig. 2 the radial profiles from Eq. (19) are given for different values of β_o, using a dimensionless radial variable $\rho = x/x_p$. As β_o increases from zero to unity, these radial profiles flatten progressively from a portion of a circle to a a uniform square profile. In Fig. 3, a graph of g as function of β_o is given. The meaning of g is shown in Fig. 3 where we plot the radial averaged value[2] $\bar{y}$ and the quantities $1-\bar{\beta}$ and $g(1-\bar{\beta})$ as functions of β_o, using $\bar{\beta} = \beta_o\bar{y}$ from Eq. (4). We observe in Fig. 3 that

$$g \sim \frac{1}{1-\bar{\beta}} \tag{22}$$

over the range of β_o of interest. The radial flux $\Gamma_x = -D_x\frac{\partial n}{\partial x}$ can be expressed, using Eqs. (12), (18), (20) and (22) as

$$\Gamma_x = \Gamma_o \cdot \left(1-y^2\right)^{\frac{1}{2}} \tag{23}$$

with the flux at the plasma edge Γ_o given by $bn_o g$. Using Eq. (22)

$$\Gamma_o \sim \left(\frac{b}{1-\bar{\beta}}\right)\frac{n_o}{x_p} \tag{24}$$

Fig. 4 shows graphs of the normalized flux $\gamma = \Gamma_x/\Gamma_o$ as a function of ρ, for different values of β_o. The peak edge flux Γ_o increases with $\bar{\beta}$ as expected since $b/(1-\bar{\beta})$ corresponds to the classical radial diffusion evaluated at the radial averaged magnetic field value $\bar{B}$ given by

$$\bar{B} = B_v\left(1-\bar{\beta}\right)^{\frac{1}{2}} \tag{25}$$

At this point we want to make two remarks concerning the edge of the radial profile in the neighborhood of $\rho = 1$. First, at $\rho = 1$, the density goes to zero although Eq. (24) shows a finite flux Γ_o. We also note from Eq. (10) that $D_z \to \infty$ as $y \to 0$. The diffusion analysis is therefore not valid as $\rho \to 1$, as can be expected since the plasma is collisionless near its outer boundary. More precisely, when the density is lowered to a certain value n_c such as $\lambda(n_c) \sim L$, one enters a free-flow regime [1] in which the axial losses are not diffusive. This corresponds to a value $y_c = n_c/n_o(z)$ and a value ρ_c such as $y(\rho_c) = y_c$ beyond which the solutions given by Eq. (19) are not valid. At this radius ρ_c, one connects into a free-flow boundary layer where the flux Γ_o is absorbed. We note from Fig. 2 that as $\beta_o \to 1$, $\rho_c \to 1$ and we are neglecting this boundary layer at the plasma edge.

Second, we observe from Fig. 2 that the radial profiles get very flat over most of the plasma cross-section as β_o approaches

unity, with increasingly sharper density gradients at the edge. This arises from the competition between the radial losses which are extremely high at the plasma center and the axial losses which are high only at the plasma edge. Presumably, transport from microinstabilities [8] or from like-particle diffusion [9] in the region of strong density gradient can increase the radial losses well over the simple classical value that is assumed here. This problem is investigated in Appendix A where we extend the diffusion analysis to a two-region plasma with different D_x in each region. The analysis shows that a much higher value of D_x near the edge does not change appreciably the solutions of Eq. (19) for high values of β_o. This interesting feature is a characteristic of the onion-skin effect which is also relevant to theta-pinch plasmas [10,11]; the axial loss increases for plasma "layers" at increasing radii. A high radial loss rate at the periphery where the axial confinement is poor anyway has little effect. This can also be seen from the radial dependence of D_z and D_x in Eqs. (10) and (12). It is also shown in Appendix A that a much higher value of D_x over a large portion of the central plasma region does not affect the results appreciably as $\beta_o \to 1$. The radial losses are already high compared to the axial losses (density profile almost completely flattened), so that it is not possible to further alter the density profile. Therefore, at high β_o, it is only in a small region near the knee of the radial profile (see Fig. 2) that the particular value of D_x is a sensitive factor. These considerations give us some confidence that taking D_x as the simple classical value is a reasonable choice.

We now consider the axial profiles. We introduce the dimensionless variables

$$\eta = n_o(z)/n_{1o}$$
$$u = z/(L/2) \tag{26}$$

into Eq. (17), with $n_{1o} = n_o(0)$. From Eqs. (3) and (6),

$$x_p(z) = x_{po}\eta^{-\frac{1}{4}} \tag{27}$$

where $x_{po} = x_p(0)$. We then have

$$\frac{d^2\eta}{du^2} = \alpha^2\eta^{3/2} \tag{28}$$

where

$$\alpha = \frac{L/2}{x_{po}}\left(\frac{b}{a}\right)^{\frac{1}{2}} g \tag{29}$$

The constant α is a measure of the relative importance of radial losses compared to axial losses. As shown in Appendix B, α can be expressed as

$$\alpha \sim \left(\frac{\tau_z}{\tau_x}\right)^{\frac{1}{2}} \tag{30}$$

where τ_z and τ_x are some average values of the axial and radial confinement times for our system. Equation (28) can be solved for the axial profile with the boundary conditions $\eta(0) = 1$ and $\eta(1) = \varepsilon$.

The value of ε, which depends on the particular sink condition at the end of the system, is not known exactly and is treated as a parameter. In typical multiple mirror experiments and reactor studies [1,3,4] the end cell density is small compared to the density near the source. We choose $\varepsilon = 0.1$ as a typical value. The axial profiles are not sensitive to the particular value of ε for the case of interest where ε is small compared to unity. Eq. (28) is solved numerically with the above boundary conditions and the axial profiles η as functions of u are plotted for different values of α in Fig. 5. The source condition is

$$\frac{S}{2} = \int \Gamma_z dA \Big|_{z=0} \tag{31}$$

where the integral is performed over the plasma cross-section A at $z = 0$. In Eq. (31) the axial flux $\Gamma_z = -D_z \frac{\partial n}{\partial z}$ can be expressed with Eqs. (1), (10) and (26) as

$$\Gamma_z = \frac{a n_{10}}{(L/2)} (1 - \beta_o y) \left(- \frac{d\eta}{du} \right) \tag{32}$$

We observe from Fig. 5 that as α increases the value of $\frac{d\eta}{du}$ at $u = 1$ tends toward zero, which implies that the axial flux Γ_z decreases with increasing α. This is consistent with particles being removed radially. However, in a real system, all particles are eventually lost axially if one takes into account the free flow boundary layer mentioned previously. Using Eq. (32), Eq. (31) becomes

$$\frac{S}{2} = \frac{an_{1o}}{(L/2)} \left(- \left. \frac{d\eta}{du} \right|_o \right) (1 - \bar{\beta})\, A_o \tag{33}$$

where A_o and $\left. \frac{d\eta}{du} \right|_o$ refer to values at $z = 0$. We recognize in Eq. (33) the reduction of plasma axial flow due to finite β in the factor $(1 - \bar{\beta})$ and the increased source requirement due to radial loss in the factor $- \left. \frac{d\eta}{du} \right|_o$. The two effects compete with each other. The variation of $- \left. \frac{d\eta}{du} \right|_o$ with α is plotted in Fig. 6.

Finally, we consider the expression for the particle confinement time τ

$$\tau = \frac{\int n \, dV}{S/2} \tag{34}$$

where $\int dV$ is a volume average for a half system. Using Eqs. (1), (26), (27) and (33) in Eq. (34), we get

$$\tau = \frac{L^2}{4a} \cdot \frac{\bar{y}}{(1 - \bar{\beta})} \cdot \frac{\int_o^1 \eta^{\frac{1}{2}} \, du}{\left(- \left. \frac{d\eta}{du} \right|_o \right)} \tag{35}$$

III. APPLICATION TO REACTOR PARAMETERS

In this section, we want to address the following questions

(i) for which values of α are radial losses important?

(ii) under which conditions can a β increase be beneficial?

A qualitative answer to (i) can be obtained directly by considering Fig. 5. We observe that the axial profile begins to be substantially altered, relative to the case $\alpha = 0$, for $\alpha \gtrsim 1$. The expressions for τ_z and τ_x in Appendix B can be used for physical insight and/or for an approximate answer to (i). A more quantitative evaluation of (i) requires the use of Eq. (35). Holding everything constant but α we define by τ_α the confinement time normalized to its value for $\alpha = 0$.

$$\tau_\alpha = \frac{\int_0^1 \eta^{\frac{1}{2}}\, du}{\left(-\frac{d\eta}{du}\Big|_0\right)} \tag{36}$$

This quantity is given as a function of α in Fig. 6. For $\alpha = 0.5$, $\tau_\alpha = 0.92$; while for $\alpha = 1$, $\tau_\alpha = 0.74$. These correpond to a reduction of confinement time due to radial losses of 8% and 24%, respectively. We therefore estimate that radial losses become significant for $\alpha \gtrsim 0.5$.

We consider now the second question (ii). The increase in axial confinement that one can achieve by increasing β is reduced by the corresponding increase of the radial losses. Neglecting the changes in axial and radial profiles in Eq. (35) the competing factors are $(1 - \bar{\beta}) \left.\frac{d\eta}{du}\right|_0$. For $\alpha \gtrsim 2$, Eq. (28) can be integrated once to get

approximately $\frac{d\eta}{du} \sim 0.89\,\alpha\,\eta^{5/4}$.

When normalized to its value for $\alpha = 0$, we obtain $\left.\frac{d\eta}{du}\right|_o \sim \alpha$. Figure 6 shows this linear dependence. Noting from Eqs. (29) and (22) that α is proportional to g and that g is inversely proportional to $(1-\bar{\beta})$, it is clear that for $\alpha \lesssim 2$, the gain due to improved axial confinement is balanced by the loss due to increased radial diffusion as one increases $\bar{\beta}$. A substantial gain is possible only for those parameters which correspond to small radial losses. For $\alpha \lesssim 0.5$, $\left.\frac{d\eta}{du}\right|_o$ has a much slower dependence on α as seen in Fig. 6, and the product $(1-\bar{\beta})\left.\frac{d\eta}{du}\right|_o$ is a decreasing function of $\bar{\beta}$. A more quantitative answer to this point would require a self-consistent optimization of the confinement time τ , including the variations in length, temperature, density and magnetic field, as one increases $\bar{\beta}$, for given fusion power and reactor Q . This is beyond the scope of this paper, since the optimization would presumably be different for each particular reactor design.

We now turn to a numerical application of the previous results to the reactor designs given by Logan [1] and Yang [3,4]. First we evaluate the quantities a and b given in Eqs. (11) and (13). We take, with T in keV, B in KG, n in cm^{-3}

$$\bar{v}_i = \left(\frac{8kT_i}{\pi m_i}\right)^{\frac{1}{2}} = 4.9\times 10^5 \left(\frac{T_i}{m}\right)^{\frac{1}{2}} \qquad (m/s)$$

$$\lambda = v_i \tau_{ii} = 1.1\times 10^{16}\,\frac{T_i^2}{n} \qquad (m) \qquad (37)$$

$$a_e = \frac{\left(T_e/m_e\right)^{\frac{1}{2}}}{\left(eB/m_e\right)} = 7.4 \times 10^{-4} \frac{T_e^{\frac{1}{2}}}{B} \qquad (m)$$

$$\nu_{ei} = 0.95 \times 10^{-10} \cdot \frac{n \log \Lambda}{T_e^{3/2}} \qquad (s^{-1}) \qquad \text{(37) cont.}$$

where m is the ratio of the ion mass to the proton mass. τ_{ii} and ν_{ei}^{-1} refer to 90° collision times, and $\log \Lambda$ is the Coulomb Logarithm. In addition, we estimate p as

$$p = \left(1 + \frac{T_e}{T_i}\right) q \qquad (38)$$

The first factor arises from the axial ambipolar potential which enhances the ion axial diffusion [12]. The second factor q corresponds to an average over a Maxwellian velocity distribution of the quantity $\lambda v/M^2$. This factor is function of the ratio of the mean free path for scattering into the loss cone angle $(\lambda^* \sim \lambda/M)$ to the cell length ℓ_c [12]. in this analysis, $\lambda^*/\ell_c = 1/4$ as seen in Eq. (7) so that q has a constant value. This value is 1.4 [1,3]. Using Eqs. (37) and (38) in Eqs. (11) and (13), we obtain

$$a = 5.5 \times 10^{21} \cdot \frac{P}{S_1} \cdot \frac{T_i^{5/2}}{n_{1o} M^2 v_1 m^{\frac{1}{2}}} \qquad (m^2/s)$$

$$b = 5.1 \times 10^{-17} \cdot \frac{n_{1o} \log \Lambda}{T_e^{\frac{1}{2}} B^2 v_1} \qquad (m^2/s) \qquad (39)$$

where n_{1o}, M_{v_1}, S_1, and B_{v_1} refer to the values at the central cell ($z = 0$). The relevant parameters of the reactor designs considered here are shown in Table I. For each design we first obtain a and b using Eq. (39) with $\log \Lambda \sim 13$. We then evaluate τ_z and τ_x using Eqs. (B6) and (B7), and determine α with Eq. (B9). Alternatively, one could use Fig. 3 and Eq. (29) to get the same value of α. The value of m corresponds to a mixture of deuterium-tritium of 50%-50% [1], 36%-64% [3] and 0%-100% [4] for the warm ions at temperature T_i. Finally, we obtain τ_α, the decrease in confinement time due to radial losses from Fig. 6. We note from Table I that for the reactor design of Logan [1] and its improved version in [3], the confinement time is reduced $\sim 20\%$ by the radial losses.

In this paper, we chose for the radial diffusion coefficient the absolute minimum value $a_e^2 \nu_{ei}$ with $v_e = (T_e/m_e)^{\frac{1}{2}}$. The real classical value could easily be twice as high. Some additional transport from microinstabilities [8] can be expected. Like-particle diffusion [9] may contribute also since it becomes comparable to the usual classical value from electron-ion collisions given above, when $x_p/a_i \sim (m_i/m_e)^{\frac{1}{4}} \sim 8$. This is the case for the designs considered here, as seen in Table I. If linked quadrupoles [13] are used to provide MHD stability some enhancement of the diffusion due to the narrow elliptical fans [9] and to the azimuthal asymmetry could be expected. We feel therefore that, for safety, a reactor design should allow for a value of α perhaps twice that found in Table I (e.g., D_x increased by a factor 4). For Logan's reactor [1], this factor of 4 reduces τ_α from 0.78 to 0.48. The improved designs with two-component plasmas [3,4] are found

to be less sensitive to radial loss, essentially because the Lawson criterion in terms of $n\tau$ is reduced compared to the one-component reactor of Logan [1]. Therefore, the values of τ_z are smaller for these designs, which decreases the relative importance of radial losses. In the last design considered [4], the hot component contributes about 70% of the total plasma pressure and allows a considerable reduction in density for the warm component. For this much less collisional plasma, radial losses are negligible ($\alpha = 0.10$ and $\tau_\alpha = 0.99$) and further improvement at higher values of $\bar{\beta}$ can be expected. To show this qualitatively, we define an overall confinement time τ^* as

$$1/\tau^* = 1/\tau_z + 1/\tau_x \tag{40}$$

where τ_z and τ_x are estimated using Eqs. (B6) and (B7), respectively. A more detailed analysis would require the use of Eq. (35). For values of $\bar{\beta}$ in the range of 0.8 to unity, the $\bar{\beta}$ dependence of τ_z and τ_x comes mainly from the factor $1 - \bar{\beta}$. We assume as a first order approximation that a, b, L and x_{po} in Eqs. (B6) and (B7) are held constant. As one increases $\bar{\beta}$, τ_z increases, τ_x decreases and a maximum value of τ^* ($d\tau^*/d\bar{\beta} = 0$) is obtained for a value $\bar{\beta}_1$ such that τ_z and τ_x are equal. Using Eqs. (B6), (B7) and (40) one obtains

$$\bar{\beta}_1 = 1 - \frac{1}{1.22} \frac{(L/2)}{x_{po}} \left(\frac{b}{a}\right)^{\frac{1}{2}} \tag{41}$$

One evaluates $\bar{\beta}_1$ for the various reactor designs by using Table I

and Eq. (39). For Logan's reactor [1], $\bar{\beta}_1 = 0.84$. No significant increase in τ^* can be obtained by increasing $\bar{\beta}$ over its design value 0.8, since τ_z and τ_x have comparable values at $\bar{\beta} = 0.8$ as seen from Table I. A similar result ($\bar{\beta}_1 = 0.86$) is obtained for the second design [3] of Table I. However, for the two-component reactor design [4], $\bar{\beta}_1 = 0.98$ and $\tau^* = 12.5$ ms compared to $\tau^* = 2.2$ ms at $\bar{\beta} = 0.8$. This improvement in confinement time can be traded for a significant reduction in density, magnetic field strength or reactor length in a self-consistent reactor optimization.

IV. CONCLUSION

We have investigated analytically a linear system where the axial diffusive loss couples to radial diffusive loss at arbitrary values of β . We assumed classical radial diffusion and complete MHD stability in a steady state system previously modeled [3]. The theory shows that as $\beta \to 1$, the radial profiles are essentially flat with sharp gradients near the plasma edge. However, it is shown that the system is not sensitive to a much higher radial diffusion rate localized at these strong density gradients, because of the poor axial confinement (onion skin effect) near the edge of the plasma. The results of the theory can be characterized in terms of a single parameter $\alpha \sim (\tau_z/\tau_x)^{\frac{1}{2}}$, and show that one can trust quantitatively a heuristic evaluation of the axial and radial loss using an effective mirror ratio M and an average magnetic field $\bar{\beta}$ given in Eqs. (9) and (25), respectively, even for values of β close to unity. Radial losses are unimportant (e.g. less than 10% decrease in confinement time)

for $\alpha \lesssim 0.5$. We showed qualitatively that some improvement in overall confinement can be made by increasing the β of a system with these small values of α . The smaller α is, the greater the improvement. Finally, it is shown that for one-component reactors [1], radial losses play a substantial role and cannot be neglected. Such designs should be optimized with the inclusion of the effect of radial losses. More recent designs [3,4] with two-component plasmas are found to be less sensitive to radial loss because of the reduced requirement in axial confinement. In one case [4], radial loss is negligible and further improvement in confinement at higher β can be expected, assuming MHD stability is preserved.

APPENDIX A

We consider now axial and radial diffusion when D_x assumes different values in two regions of the plasma cross-section. We take for regions 1 and 2

$$b_1 = k_1^2 b \qquad 0 \leq \rho \leq \rho_o$$

$$b_2 = k_2^2 b \qquad \rho_o \leq \rho \leq 1 \tag{A1}$$

where k_1 and k_2 are two arbitrary constants and b is defined in Eq. (13). Equation (16) can then be integrated twice in each region as done previously and the four constants of integration are determined with the following boundary conditions. $y_1(0) = 1$, $y_2(1) = 0$, $y_1 = y_2$ at ρ_o and $\frac{\partial y_1}{\partial x} = \frac{\partial y_2}{\partial x}$ at ρ_o . The expression for g in Eq. (21) now becomes

$$g = \frac{k_2}{\beta_o}\left\{B_2 + \left\{\begin{array}{ll} \dfrac{1}{\sqrt{-A_2}} \arcsin\left(\dfrac{1+A_2}{\beta_o}\right) & A_2 < 0 \\ -\dfrac{1}{\sqrt{A_2}} \log\left(2\left(1 + A_2 + \sqrt{A_2(1+A_2)}\right)\right) & A_2 > 0 \end{array}\right\}\right\}, \tag{A2}$$

where

$$B_2 = \frac{\beta_o}{k_2} u_o - \arcsin\left(\frac{y_o\beta_o}{\sqrt{1+A_2}}\right) +$$

$$+ \begin{cases} -\dfrac{1}{\sqrt{-A_2}} \arcsin\left[\dfrac{A_2 + 1 - y_o\beta_o}{(1-y_o\beta_o)\beta_o}\right] & A_2 < 0 \\ \dfrac{1}{\sqrt{A_2}} \log\left[\dfrac{2A_2 + 2(1-y_o\beta_o) + 2(k_2/k_1)\beta_o\sqrt{A_2(1-y_o^2)}}{1-y_o\beta_o}\right] & A_2 > 0 \end{cases} \qquad \text{(A3)}$$

where u_o and $y_o = y(\rho_o)$ are related by

$$\arcsin y_o + \frac{1}{\sqrt{1-\beta_o^2}} \arcsin\left(\frac{\beta_o - y_o}{1-y_o\beta_o}\right) = \frac{\beta_o}{k_1} u_o - \frac{\pi}{2}\left(\frac{1}{\sqrt{1-\beta_o^2}} - 1\right) \qquad \text{(A4)}$$

and

$$A_2 = \beta_o^2\left(k_2/k_1\right)^2\left(1-y_o^2\right) - \left(1-\beta_o^2 y_o^2\right) \qquad \text{(A5)}$$

Consider first the case of a higher radial diffusion near the plasma edge. As a typical example, we take $\rho_o = 0.8$ and $\beta_o = 0.95$. k_1 is unity and k_2 varies. For each value of k_2, we first determine y_o from Fig. 2 since the solution in region 1 corresponds to those graphs. Then u_o is obtained from Eq. (A4), A_2 from Eq. (A5), B_2 from Eq. (A3) and g from Eq. (A1). We normalize g to the value $(k_1 = k_2 = 1)$ given by Eq. (21). The results are shown in Fig. 7, curve (a). We note that a much higher diffusion rate near the plasma edge does not change appreciably ($\lesssim 10\%$) the value of g. Then α, which is proportional to g, also does not change appreciably.

We consider now the case of a high radial diffusion over the central region of the plasma cross-section. For example, $\rho_o = 0.5$ and $\beta_o = 0.95$. k_2 is unity k_1 varies. We obtained g as previously and the results are given in Fig. 7, Curve (b). We note that in the limit of $k_1 \to \infty$, $g \to 1+\rho_o$. This may be expected since in that limit $y_o = 1$ and the radial profile is the same as in Fig. 2 except for a flat region of extent ρ_o .

APPENDIX B

To evaluate in a heuristic way the relative importance of radial losses compared to axial losses for the system considered in this paper, we define "average" confinement times against radial and axial losses, τ_x and τ_z, respectively, with

$$\tau_z = \frac{(L/2)^2}{2D_z} \tag{B1}$$

$$\tau_x = \frac{\bar{x}_p^2}{2D_x} \tag{B2}$$

where $\bar{x}_p$ is the axial averaged value of the plasma radius and D_z and D_x the radial averaged values of the diffusion coefficients. From Eq. (27), assuming the linear axial profile corresponding to $\alpha \ll 1$, we get

$$\bar{x}_p = 1.21\, x_{po} \tag{B3}$$

Using Eqs. (10) and (12), we estimate,

$$D_z = a(1 - \bar{\beta}) \tag{B4}$$

$$D_x = b/(1 - \bar{\beta}) \tag{B5}$$

so that Eqs. (B1) and (B2) become

$$\tau_z = \frac{(L/2)^2}{2a(1 - \bar{\beta})} \tag{B6}$$

$$\tau_x = \frac{1.5x_{po}^2 (1 - \bar{\beta})}{2b} \tag{B7}$$

The constant α defined in Eq. (29) can be expressed as a function of τ_z and τ_x if we use, for $\beta_o \geq 0.8$

$$g \simeq \frac{0.93}{(1 - \bar{\beta})} \tag{B8}$$

This expression is essentially the same as in Eq. (22). The factor 0.93 is derived from Fig. (3). We use Eqs. (B6), (B7) and (B8) in Eq. (29) to obtain

$$\alpha = 1.12 \left(\frac{\tau_z}{\tau_x} \right)^{\frac{1}{2}} \tag{B9}$$

which relates the value of α in this paper to the estimates of the axial and radial times τ_z and τ_x, given by Eqs. (B6) and (B7), respectively.

ACKNOWLEDGMENTS

It is a pleasure to acknowledge the benefit of useful discussions with A. J. Lichtenberg. This research was supported by U.S. DOE Contract EY-76-S-03-0034-PA215 and NSF Grant ENG78-09424.

REFERENCES

[1] Logan, B. G., Brown, I. G., Lichtenberg, A. J., and Lieberman, M. A., Phys. Fluids 17 (1974) 1302

[2] Budker, G. I., Mirnov, V. V., and Ryutov, D. D., Zh. Ehksp. Teor. Fiz. Pis. Red 14 (1971) 320

[3] Yang, S. T. and Lieberman, M. A., Nucl. Fusion 17 (1977) 697

[4] Yang, S. T. and Lieberman, M. A., Nucl. Fusion 18 (1978) 965

[5] Logan, B. G., Lichtenberg, A. J., Lieberman, M. A., and Makhijani, A., Phys. Rev. Lett. 28 (1972) 144

[6] Mirnov, V. V. and Ryutov, D. D., Nucl. Fusion 12 (1972) 627

[7] Lichtenberg, A. J. and Lieberman, M. A., Nucl. Fusion 16 (1976) 532

[8] Steinhauer, L., Phys. Fluids 21 (1978) 230

[9] Tuszewski, M. and Lichtenberg, A. J., Phys. Fluids 20 (1977) 1263

[10] Steinhauer, L., Phys. Fluids 19 (1976) 738

[11] Bodin, H. A. B., McCartan J., Pasco, I. K., and Schneider, W. H., Phys. Fluids 15 (1972) 1341

[12] Makhijani, A., Lichtenberg, A. J., Lieberman, M. A., and Logan, B. G., Phys. Fluids 17 (1974) 1291

[13] Riordan, J. C., Lichtenberg, A. J., and Lieberman, M. A., Nucl. Fusion 19 (1979) 21

FOOTNOTES

[1] Nonadiabatic effects [7] that can in principle allow a much less collisional plasma are not considered in this paper.

[2] We use here the Cartesian average $\bar{y} = \int_0^1 y(\rho)d\rho$. In addition, $\bar{y}$ is normalized to its value for $\beta_o = 0$ in Fig. 3.

Reference Number	Q	T_e (KeV)	T_i (KeV)	n_{10} ($\times 10^{-16}$ cm^{-3})	B_{v1} (KG)	$\bar{\beta}$	M_{v1}	L (m)	X_{po} (cm)	$\frac{\bar{x}_p}{a_i}$ (a) (b)	P	S_1	m	τ_z (ms)	τ_x (ms)	α	τ_α
1	2	4.5	4.5	9	200	0.8	1.5	400	1.5	11	2.8	0.64	2.5	31	48	0.90	0.78
3 (c)	2.8	5	5	6.5	170	0.8	1.7	440	1.6	9	2.8	0.73	2.64	32	58	0.83	0.81
4	2.1	5.6	3.1	0.65	93	0.8 (d)	1.7	230	2	8	3.9	0.73	3	2.2	285	0.10	0.99

(a) radius for $P_{net} = P_{recirc} = 3000$ MWe

(b) axial average value of the ratio of plasma radius x_p to ion gyroradius a_i

(c) one-component reactor design parameters of Table I in [3]. Two-component reactor designs are also considered in [3].

(d) $\bar{\beta}$ corresponds to the total pressure; hot beam and warm plasma.

TABLE I.

Comparison of various reactor designs.

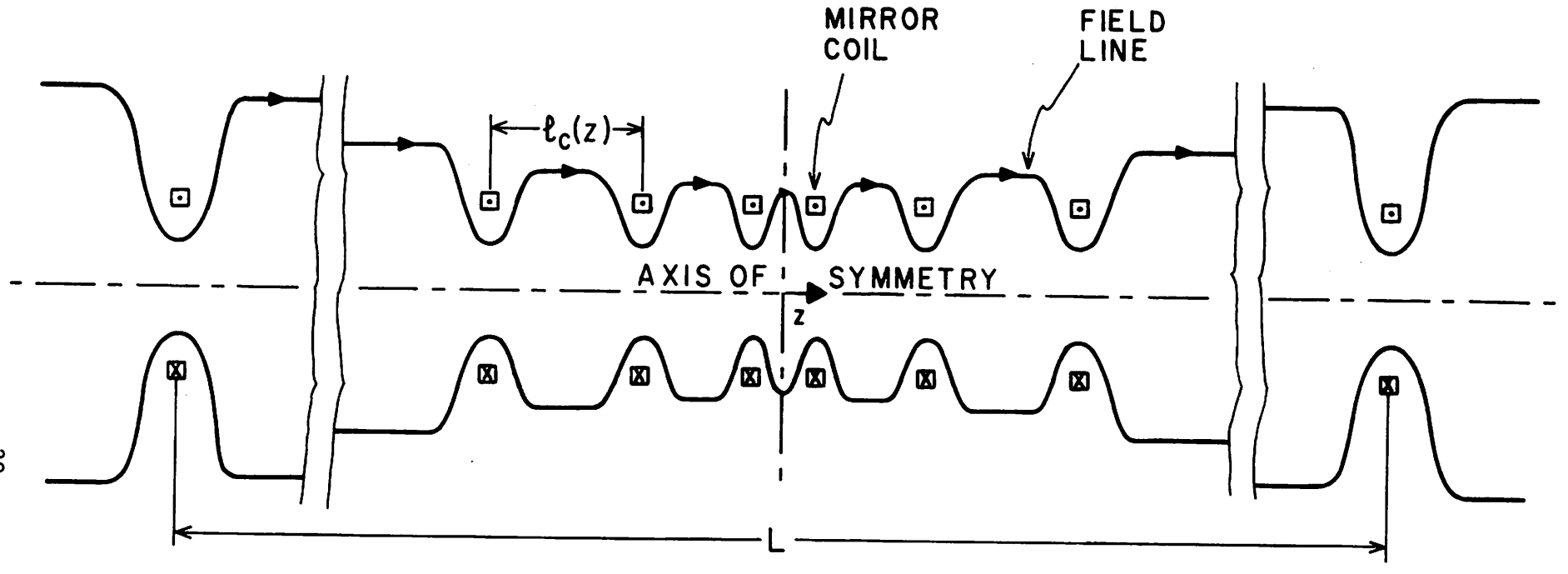

FIG. 1 Magnetic field variation for a multiple mirror reactor

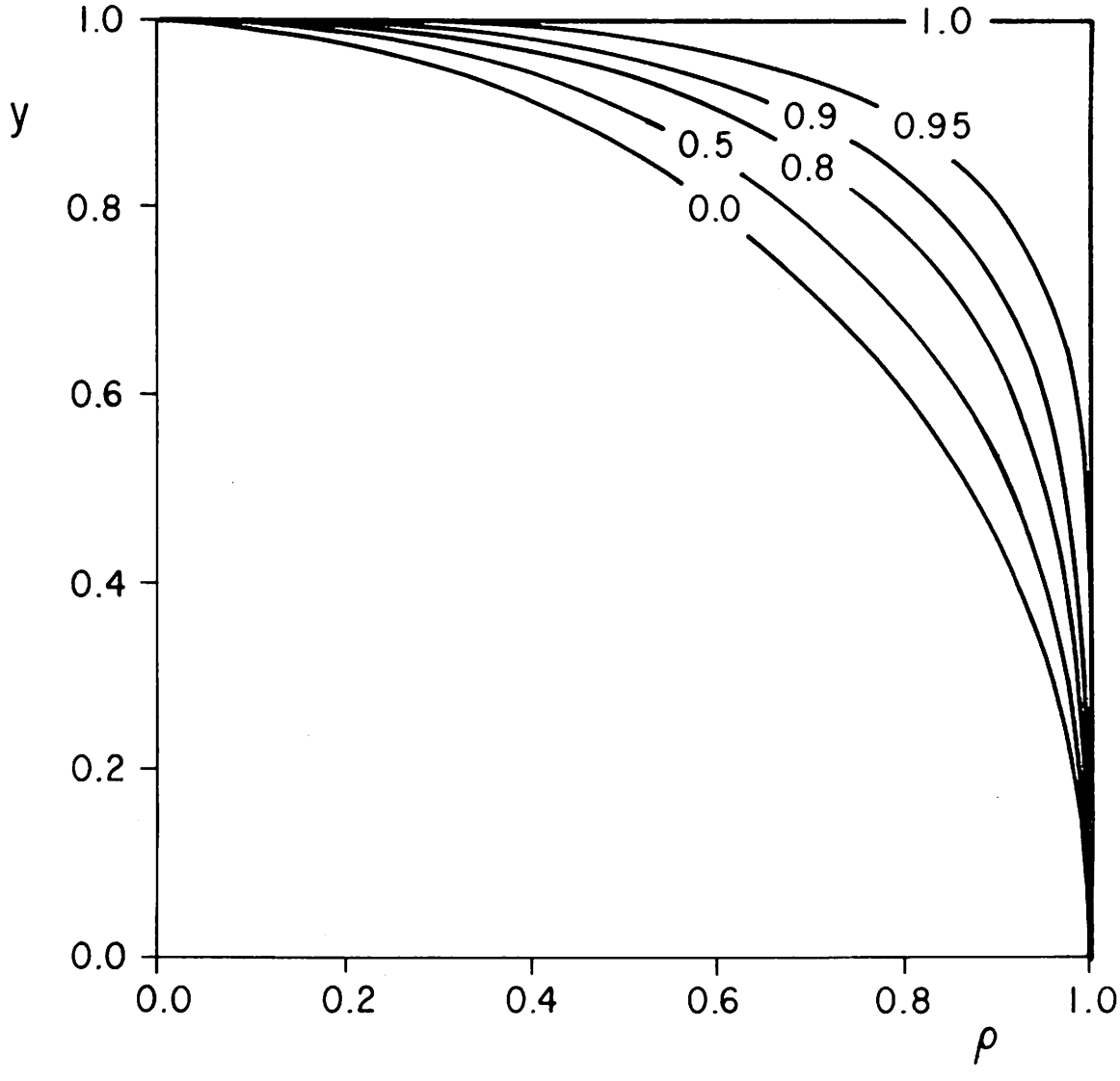

FIG. 2 Normalized radial profiles $y(\rho)$ for different values of β_o

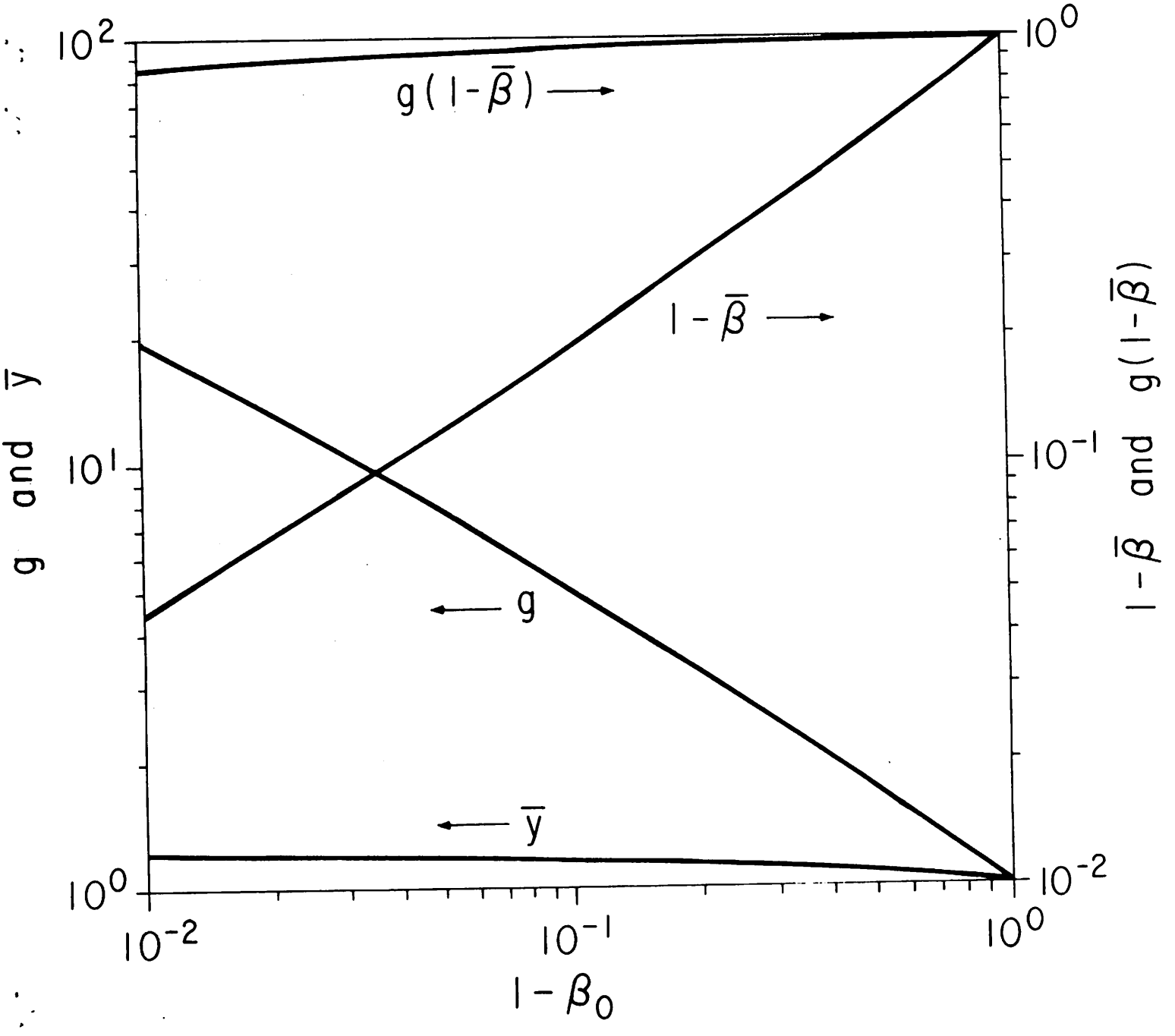

FIG. 3 Averaged density $\bar{y}$, average β , $1-\bar{\beta}$, g and $g(1-\bar{\beta})$ as function of β_o

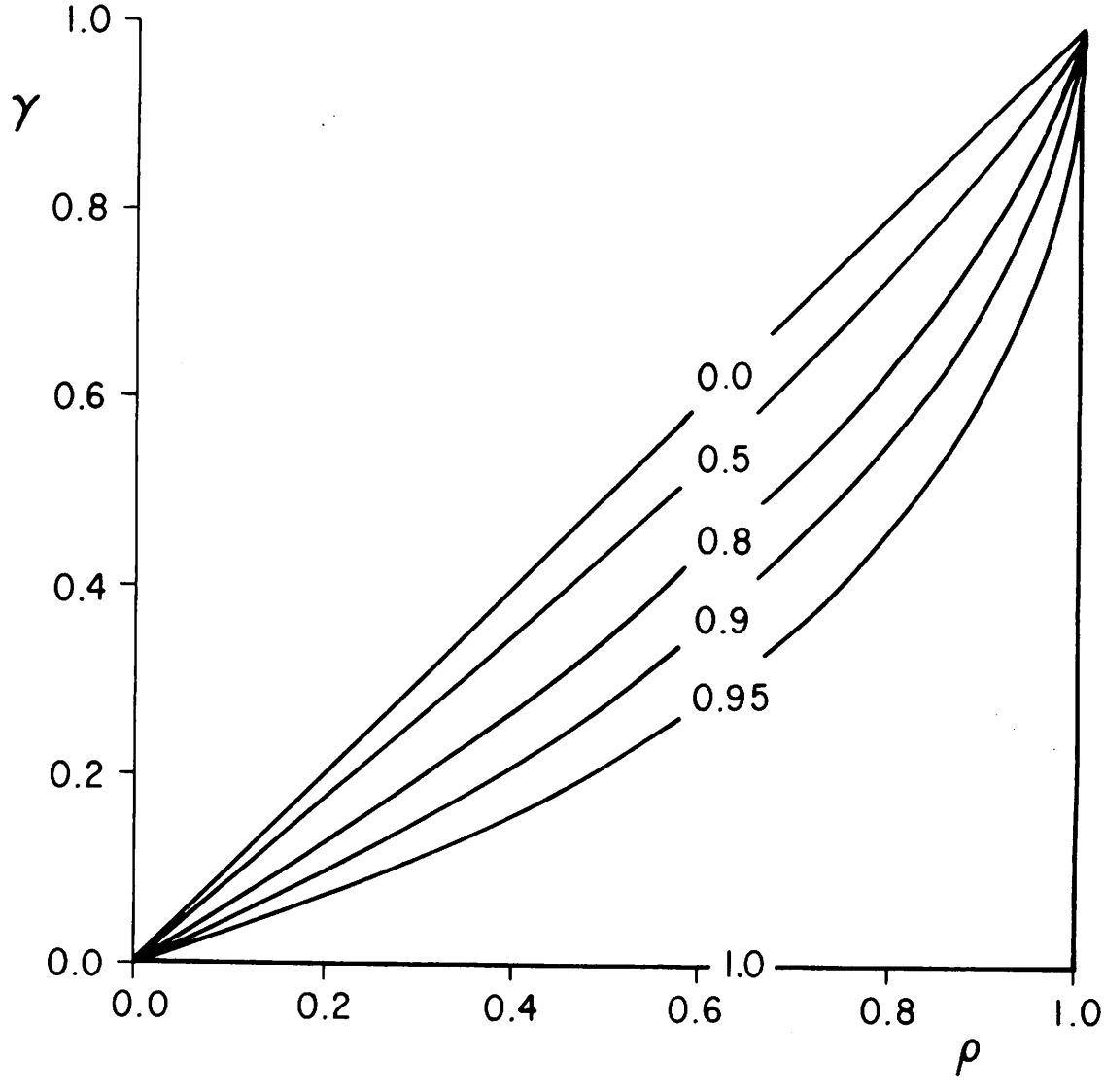

FIG. 4 Normalized radial fluxes $\gamma(\rho)$ for different values of β_o

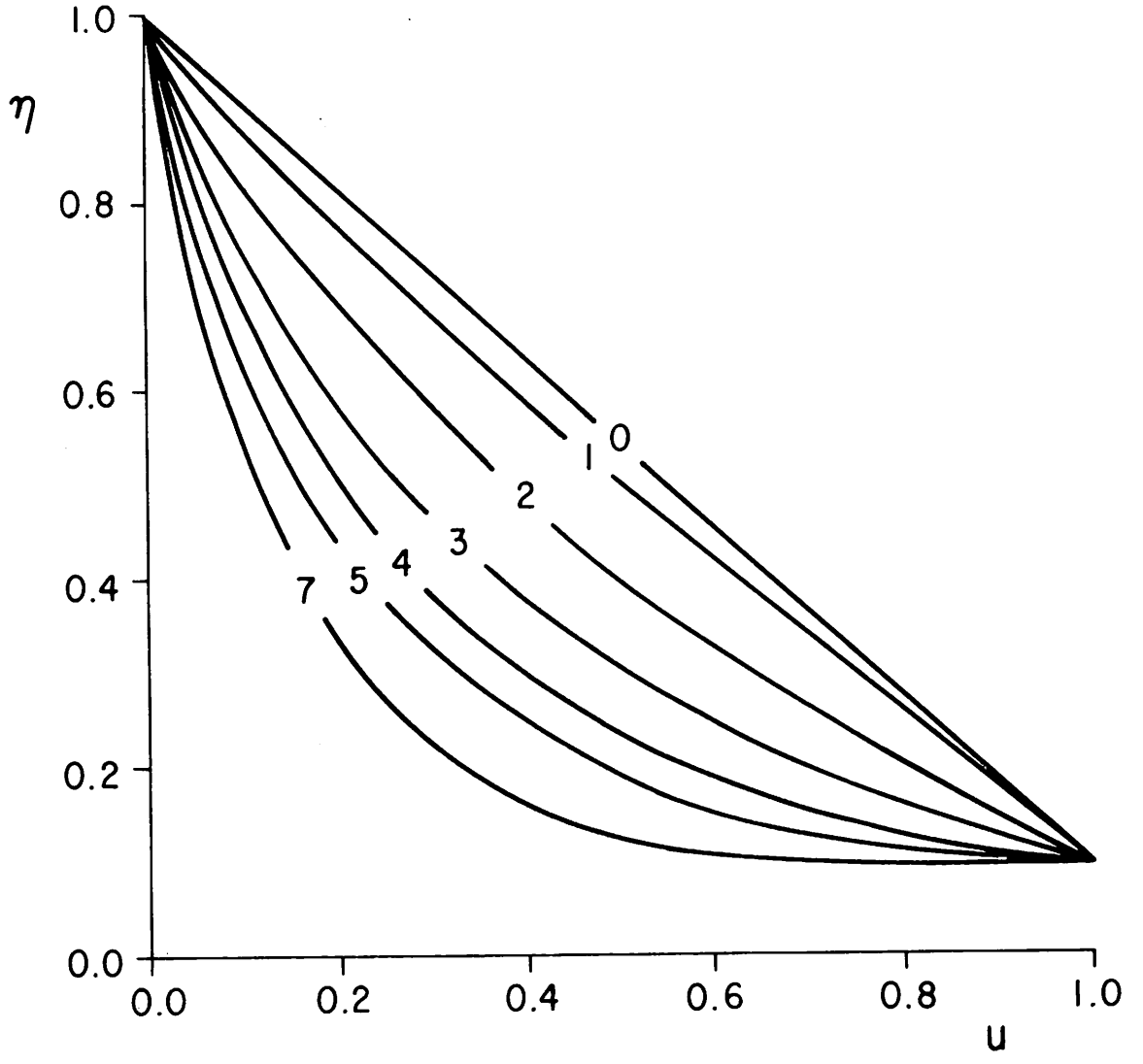

FIG. 5 Normalized axial profiles $\eta(u)$ for different values of α

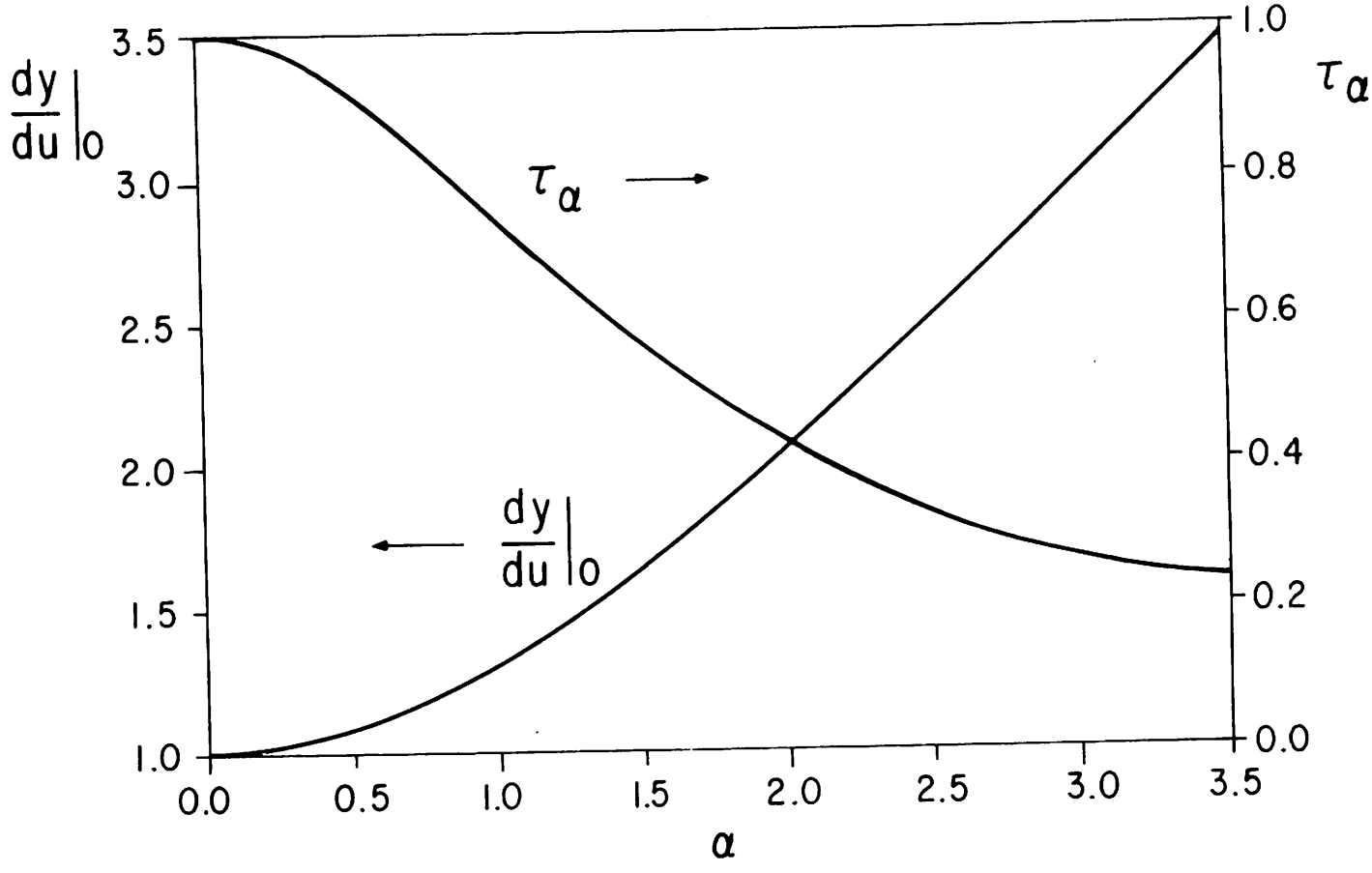

FIG. 6 Source intensity $-\left.\frac{d\eta}{du}\right|_o$ and confinement time τ_α normalized to their values at $\alpha = 0$, as functions of α

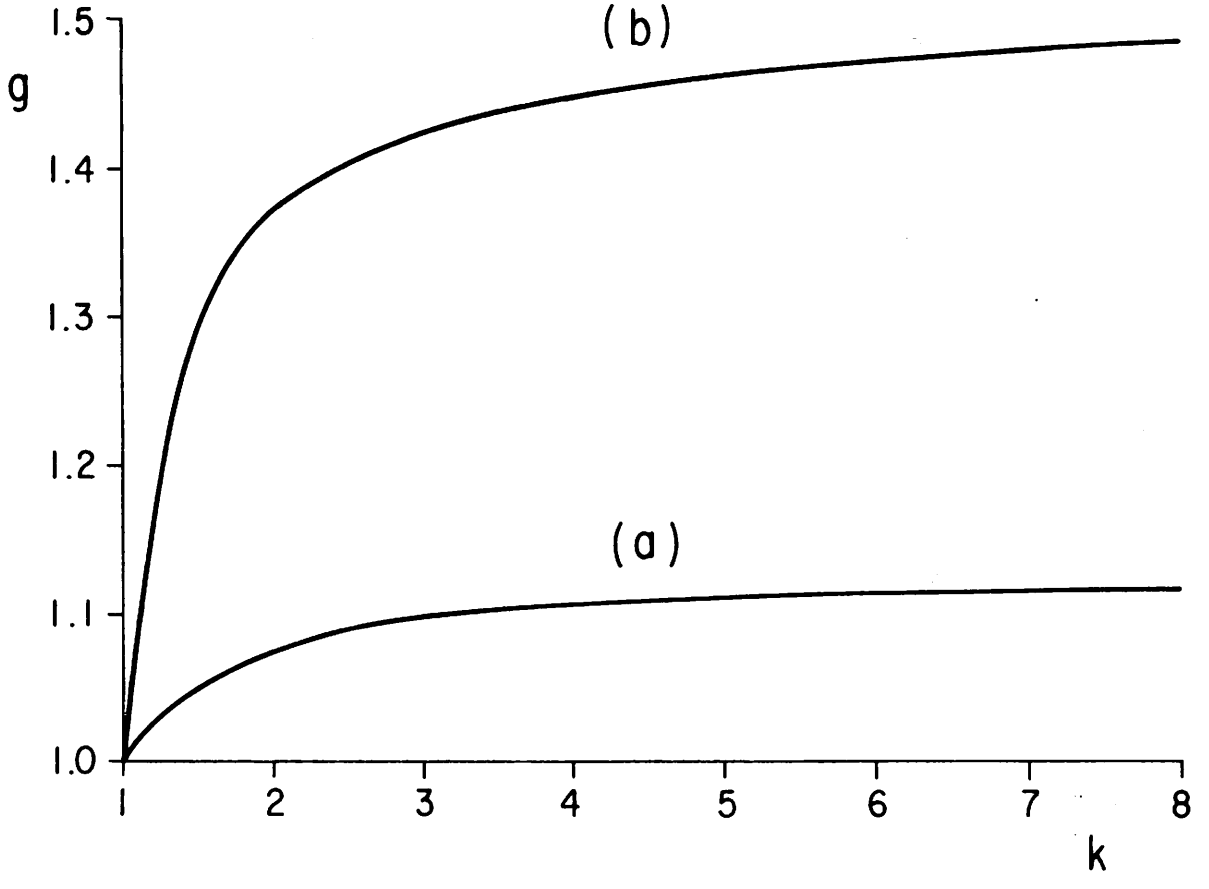

FIG. 7 Relative increase of $g(\alpha)$ compared to the case $k_1 = k_2 = 1$

(a) Enhanced diffusion at the plasma edge ($k_1 = 1$, $k_2 = k$, $\beta_o = 0.95$, $t_o = 0.8$)

(b) Enhanced diffusion at the plasma center ($k_1 = k$, $k_2 = 1$, $\beta_o = 0.95$, $t_o = 0.5$)